

[*Progress in Biological Chirality*, G.Palyi, C.Zucchi & L.Caglioti [Eds], Oxford: Elsevier, 2004. pp.137-151]

## Chapter 11

# Chiral Crystal Faces of Common Rock-Forming Minerals

Robert M. Hazen

*Geophysical Laboratory and NASA Astrobiology Institute, Carnegie Institution of Washington, 5251 Broad Branch Road NW, Washington, DC 20015-1305, USA*

---

### 1. Introduction

Chiral crystalline surfaces provide effective environments for chiral molecular discrimination in both natural and industrial contexts [1]. Such surfaces have been cited for almost 70 years in reference to their possible role in the origins of biochemical homochirality [2-7]. In the past decade, furthermore, chiral crystal surfaces have received attention for their potential applications in the chiral selection and purification of pharmaceuticals and other molecular products [8 -12].

Many recent studies have focused on the behavior of chiral surfaces of cubic close-packed (CCP) metals, including copper, silver, gold and platinum [13-23]. Single crystals of these metals, which can be modified by cutting, polishing and annealing faces with high Miller indices, display surfaces with chiral “kink” sites, even though the three-dimensional CCP structure is intrinsically achiral. Theoretical studies of these metal surfaces have demonstrated the potential for significant differences in adsorption energies of D - versus L-molecules [14,21-23], while experiments provide indirect evidence for chiral selectivity [13,15-19].

Considerably less attention has been focused on the wide variety of chiral oxide and silicate mineral surfaces, which are ubiquitous in Earth’s crust. Such surfaces provide the most abundant and accessible local chiral geochemical environments, and thus represent logical sites for the prebiotic chiral selection and organization of essential biomolecules. This chapter summarizes the geological occurrence, physical properties, crystal morphology and surface structures of some of the most common of these natural surfaces, including crystal faces of quartz ( $\text{SiO}_2$ ), alkali feldspar  $[(\text{Na,K})\text{AlSi}_3\text{O}_8]$ , clinopyroxene  $[(\text{Ca,Mg,Fe})\text{SiO}_3]$ , and calcite ( $\text{CaCO}_3$ ). One or more of these minerals is present in most common rocks in Earth’s crust, as well as on the Moon, Mars and other terrestrial bodies, so chiral crystal environments are correspondingly ubiquitous [24,25].

## 2. Chiral Environments on Mineral Surfaces: General Considerations

Many natural crystals are “euhedral” – bounded by a set of planar faces. These natural crystal growth surfaces, or “terminations,” may be represented as the intersection of a plane with a three-dimensional periodic atomic structure. Such surfaces are usually defined in terms of a set of three integers, known as Miller indices, which relate the orientation of the terminal plane to integral intercepts of the three crystallographic axes [26,27]. For a given unit cell, every possible planar termination has a unique corresponding set of Miller indices.

A chiral crystal surface is defined as any terminal arrangement of atoms that cannot be superimposed on its reflection in a mirror perpendicular to the surface. Such crystal surfaces display three common types of chiral environments. Some atomic surfaces are chiral because the periodic two-dimensional structure of the exposed surface lacks mirror symmetry (Figure 1a). These surface atoms may be coplanar or they may display significant topography. In either case such a surface, if chiral, is not superimposable on its reflection in a perpendicular mirror.

Many crystal surfaces possess perpendicular mirror symmetry and thus are inherently achiral. Nevertheless, such faces often feature steps in the atomic structure that intersect the mirror symmetry operator at other than right angles (Figure 1b). Under these circumstances, local environments immediately along the step edge are chiral, even though most of the crystal face is achiral.

A third type of chiral environment, a local “chiral center,” may occur on any crystal face. Chiral centers commonly arise on surfaces in which both planar regions and steps possess mirror symmetry, as in the case of face-centered cubic metals. In these cases the steps may be “kinked” to provide a chiral center at the kink site (Figure 1c) [13].

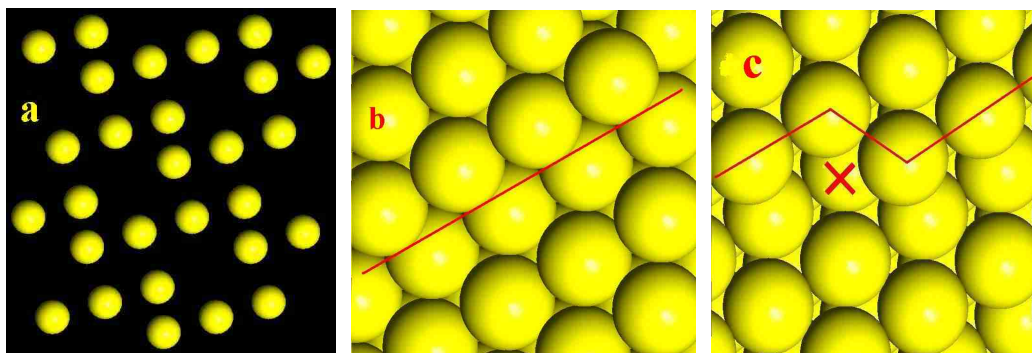


Figure 1. Crystals commonly display three types of chiral surface features, illustrated here in idealized drawings. (a) A periodic two-dimensional chiral arrangement of atoms in a plane; these atoms may be coplanar or they may occur at slightly different heights. (b) A terrace step that is chiral along a step edge (red line) (c) A kink site that provides a chiral center (X).

Two distinct types of symmetry conditions lead to chiral crystal surfaces. A few minerals are inherently chiral because their crystallographic space group lacks any of the so-called “improper” symmetry operators, including mirrors, glide planes, an inversion center or a roto-inversion operator [26,27]. Thus, in minerals such as quartz (space group  $P3_121$  or  $P3_221$ ) every surface is chiral and there exist so-called left- and right-handed structural variants, which are not superimposable and thus related to each other by mirror symmetry [28,29].

Most minerals possess space group symmetries that incorporate at least one mirror symmetry operator, and thus the mineral is intrinsically achiral. Nevertheless, as noted above, a crystal termination will be chiral if no perpendicular mirror symmetry operator intersects that termination. This condition is met by one or more common crystal growth surfaces of many common rock-forming minerals. These faces, which have received little attention in terms of their chiral properties, provide the primary focus of this chapter.

In addition to chiral planes, most crystal surfaces possess etch pits, growth steps, twin boundaries, dislocations or other nonperiodic features that provide numerous local chiral centers on an otherwise achiral surface environment. These ubiquitous local chiral features may have been important in fostering chiral molecular processes, but they are not in the scope of this review.

Before examining the characteristics of specific chiral mineral surfaces, it is important to emphasize that all of these natural chiral surface environments occur in both left- and right-handed variants in approximately equal proportions. No evidence exists for an enantiomeric excess of any chiral mineral feature [30,31]. Nevertheless, the widespread occurrence of local chiral environments provided the prebiotic Earth with innumerable sites for experiments in chiral selection and organization – experiments that may have led, through a process of chiral amplification [32-35], to a fortuitous, self-replicating homochiral entity. These minerals, furthermore, represent an untapped library of chiral surfaces for possible industrial applications.

The following section examines four common groups of rock-forming minerals that routinely display chiral crystal growth faces.

### **3. Common Chiral Crystal Faces of Minerals**

#### *3.1 Quartz*

Quartz ( $\text{SiO}_2$ , trigonal space group  $P3_121$  or  $P3_221$ ,  $a = 4.91 \text{ \AA}$ ,  $c = 5.41 \text{ \AA}$ ) is the predominant colorless mineral in most beach sand and is a principal component of many igneous, sedimentary and metamorphic rocks. Quartz is the only common rock-forming mineral that occurs in both right and left-handed variants. This structural distinction arises from the silicate framework that incorporates either right- or left-handed helices of corner-linked  $\text{SiO}_4$  tetrahedra [28,36].

Three common crystal faces, illustrated in Figure 2, provide important chiral surfaces for study [37]: the ubiquitous (100) prism faces (denoted  $m$  in Figure 2), the dominant (101) rhombohedral termination ( $r$ ), and the (011) rhombohedral termination ( $z$ ), which is typically less well developed than (101). Note, however, that these three crystal forms are generally insufficient to distinguish right- from left-handed specimens. This distinction can be made, however, if the (111) and (511) faces ( $s$  and  $x$ , respectively) are present (Figures 2a and 2b, respectively).

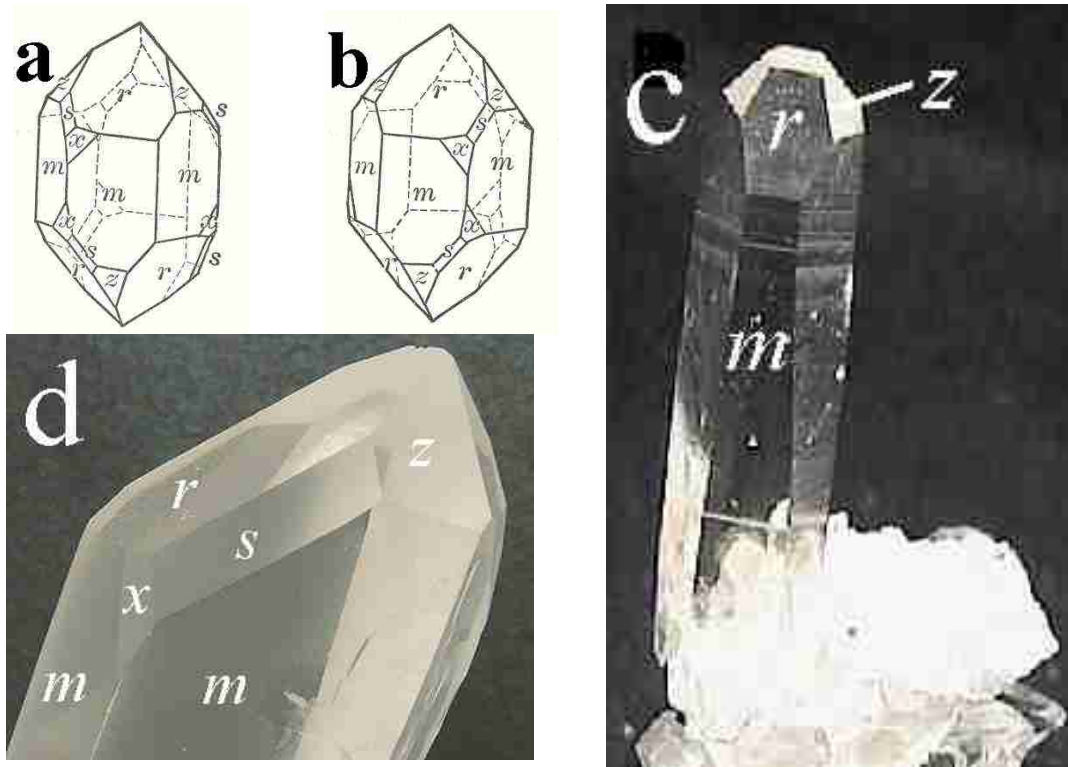


Figure 2. Common crystal forms of quartz include the hexagonal prism  $m$  (100), the dominant rhombohedron  $r$  (101) and the secondary rhombohedron  $z$  (011). Left- and right-handed quartz (a and b, respectively) may be distinguished by two additional forms, denoted  $s$  (111) and  $x$  (511). Most crystals, such as the 3.2 -cm diameter specimen from Montgomery County, Arkansas (c), display only the  $m$ ,  $r$ , and  $z$  faces. Less common specimens, such as the 3.5 -cm diameter right-handed crystal from Betroka, Madagascar (d), develop the additional forms.

The surface structures of the three common quartz forms ( $m$ ,  $r$ , and  $z$ ), while all chiral, are markedly different from each other, as illustrated in Figure 3. Above the point of zero charge of quartz ( $\text{pH} \approx 2.5$ ), the quartz surface charge is negative [38-40]. In addition, silicon atoms typically remain tetrahedrally coordinated, so

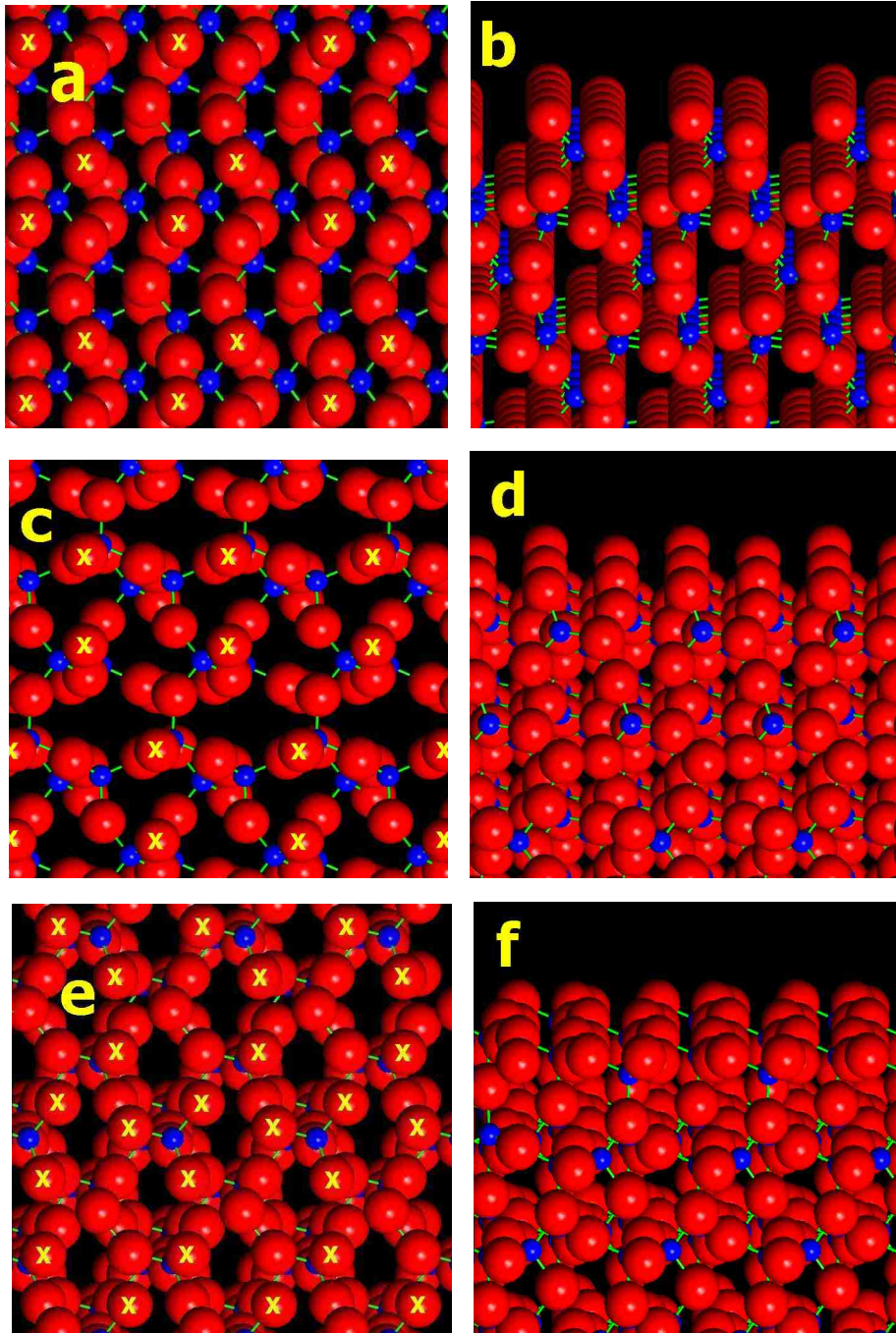


Figure 3. The (100), (101) and (011) surface structures of quartz ( $\text{SiO}_2$ ), viewed from above (a, c, and e, respectively) and tilted  $3^\circ$  from horizontal (b, d, and f, respectively). Oxygen and silicon atoms are shown in red and blue, respectively. Positions of terminal oxygen atoms are indicated by yellow Xs. In each drawing the c-axis projection is vertical and each drawing presents an area  $15 \times 15 \text{ \AA}$ .

oxygen atoms (perhaps bonded to H, depending on pH) are expected to define the crystal terminations [41,42]. Given this assumption, the surface structures of the (100), (101), and (011) faces are well constrained.

The (100) prism face has zigzag bands of oxygen atoms separated by channels approximately 1.5 Å wide and 2.0 Å deep (Figure 3a). Note, therefore (Figure 3b), that the “surface” oxygen atoms are not coplanar. This feature is of critical importance in modeling surface interaction of quartz and other minerals. By contrast, the (101) face can be modeled with a more planar surface with a distribution of oxygen atoms that is much closer to an achiral array (Figure 3c and d). The (011) face presents yet a different character, with a denser chiral array of surface oxygen atoms (Figure 3e and f).

These three faces also differ in the coordination of terminal oxygen atoms. On the (101) face all oxygen atoms are coordinated to a single silicon atom, whereas all oxygen atoms on the (011) face are coordinated to two silicon atoms. The (100) face, by contrast, features both one - and two-coordinated oxygen atoms

These marked differences in surface distribution of oxygen atoms explain, for example, the dramatically different adsorption characteristics of hematite ( $\text{Fe}_2\text{O}_3$ ) on (101) versus (011) rhombohedral faces of some natural quartz crystals (Figure 4). These differences also point to the necessity of studying any surface interactions, such as selective adsorption of organic molecules, on individual faces rather than on powdered material. Given the striking differences in surface structures, the adsorption behavior of a molecule on one surface can bear little relationship to adsorption on any other face.



Figure 4. Hematite ( $\text{Fe}_2\text{O}_3$ ) preferentially deposits on (101) faces of quartz, while (011) faces remain largely uncoated (~1-mm diameter crystals from Paterson, New Jersey). This phenomenon results from significant differences in the surface structures of these two rhombohedral faces (see Figure 3c and d versus 3e and f).

### 3.2 Alkali Feldspar

Feldspars, including the alkali feldspar series  $(\text{Na,K})\text{AlSi}_3\text{O}_8$  and the plagioclase feldspar series  $(\text{NaSi,CaAl})\text{AlSi}_2\text{O}_8$ , are among the most common rock-forming minerals in Earth's crust [24,25]. These framework aluminosilicates are major constituents of most igneous rocks and they provide the principal repositories of alkali and alkaline earth cations. Feldspars form significant fractions of many sedimentary and metamorphic rocks, as well.

A variety of alkali feldspars, including both orthoclase (Figure 5a:  $\text{KAlSi}_3\text{O}_8$ , monoclinic space group  $C2/m$ ,  $a = 8.56 \text{ \AA}$ ,  $b = 13.0 \text{ \AA}$ ,  $c = 7.19 \text{ \AA}$ ,  $\beta = 89.1^\circ$ ) and albite (Figure 5b:  $\text{NaAlSi}_3\text{O}_8$ , triclinic space group  $C\bar{1}$ ,  $a = 8.14 \text{ \AA}$ ,  $b = 12.8 \text{ \AA}$ ,  $c = 7.16 \text{ \AA}$ ,  $\alpha = 94.3^\circ$ ,  $\beta = 116.5^\circ$ ,  $\gamma = 87.7^\circ$ ), commonly have well-developed (110) faces. This form occurs in enantiomeric pairs in many natural crystals (Figure 5c).

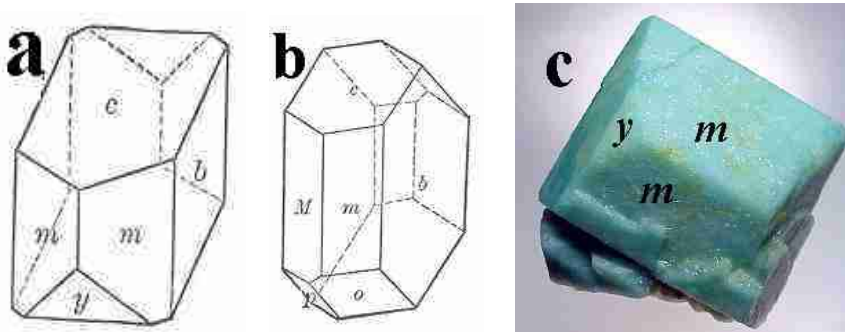


Figure 5. Common crystal faces of feldspar include the chiral form  $m$  (110), which is often well developed in orthoclase (a) and albite (b). The 7 - x 7-cm specimen of alkali feldspar (c) from Ethiopia displays these faces.

The surface structures of feldspar are less well constrained than those of quartz because of uncertainties in the terminal oxygen configurations near alkali cations. It is likely, for example, that oxygen coordination of alkali cations near the crystal surface in an aqueous environment will vary as a function of pH. Uncertainty also arises from the occurrence of different ordered distributions of silicon and aluminum atoms in tetrahedral coordination, as well as the facile exchange of alkali and alkaline earth cations between the crystal surface and aqueous solution [43].

Given these uncertainties, one possible configuration of oxygen atoms at the (110) chiral surface is illustrated in Figure 6. In this example of an orthoclase surface structure with potassium atoms retaining their full 7-coordination, oxygen atoms are arrayed in rows approximately parallel to  $[001]$ , as illustrated in Figure 6a. This surface displays significantly nonplanar topography as a consequence of the oxygen atoms selected (Figure 6b). A different choice of terminal oxygen atoms (for example removing the highest rows of atoms in Figure 6b) would significantly increase the surface exposure of positively-charged alkali cations.

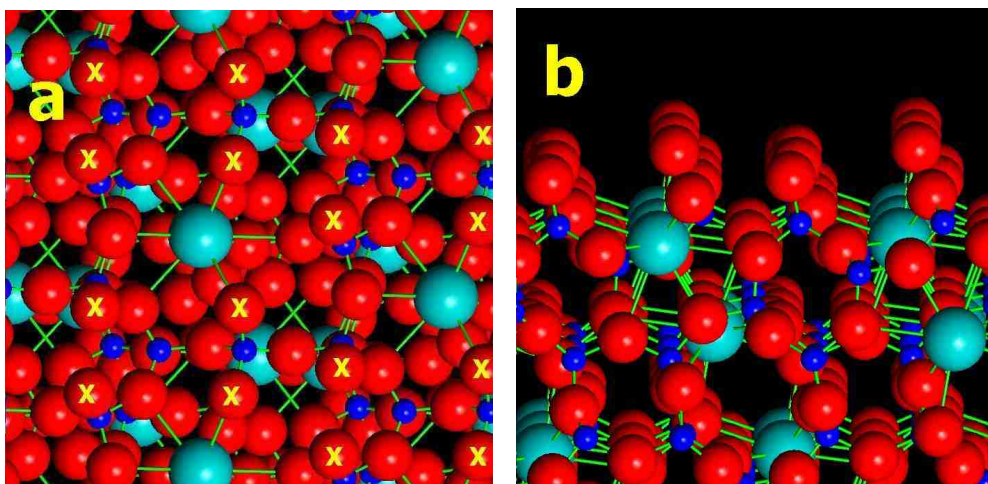


Figure 6. One possible (110) chiral surface structure of orthoclase, which is a member of the alkali feldspar group. Silicon, oxygen and potassium atoms are shown in blue, red and turquoise, respectively. Terminal oxygen atoms are marked with yellow Xs. The [001] axis is vertical and the area is 15 x 15 Å. Note that terminal oxygen atoms are chosen in this model so that potassium is fully coordinated, which effectively shields potassium atoms from the surface.

### 3.3 Clinopyroxene

Clinopyroxenes, the most common of all ferromagnesian rock-forming minerals, incorporate a diverse group of species with the general formula  $(\text{Ca}, \text{Mg}, \text{Fe})\text{SiO}_3$  [36]. Pyroxenes are major components in many igneous and metamorphic rocks in both the Earth's crust and upper mantle. They occur commonly in both orthorhombic and monoclinic varieties, but it is the latter that most commonly offer chiral crystal growth faces. The most common clinopyroxene structure, as typified by the mineral diopside ( $\text{CaMgSi}_2\text{O}_6$ , monoclinic space group  $C2/c$ ,  $a = 9.75 \text{ \AA}$ ,  $b = 8.90 \text{ \AA}$ ,  $c = 5.25 \text{ \AA}$ ,  $\beta = 105.6^\circ$ ), features chains of corner-linked silicate tetrahedra that are cross-linked by divalent Mg and Ca cations in 6- and 8-coordination, respectively.

The most common chiral clinopyroxene face is the ubiquitous (110) perfect cleavage plane, which is designated  $m$  (Figure 7a). This face also occurs on crystals, occasionally in combination with the (111), (221) and  $(\bar{2}21)$  chiral faces [37]. In addition, four (110)-type faces often combine with pairs of (100) and (010) faces to form an 8-sided crystal prism (Figure 7c). Such elongated crystals, which parallel the silicate chain, represent a distinctive morphology of clinopyroxenes. The fact that the (110) surface is also a perfect cleavage surface in clinopyroxene raises the possibility of obtaining large, freshly exposed chiral surfaces from cleaved samples for studies of chiral molecular interactions.

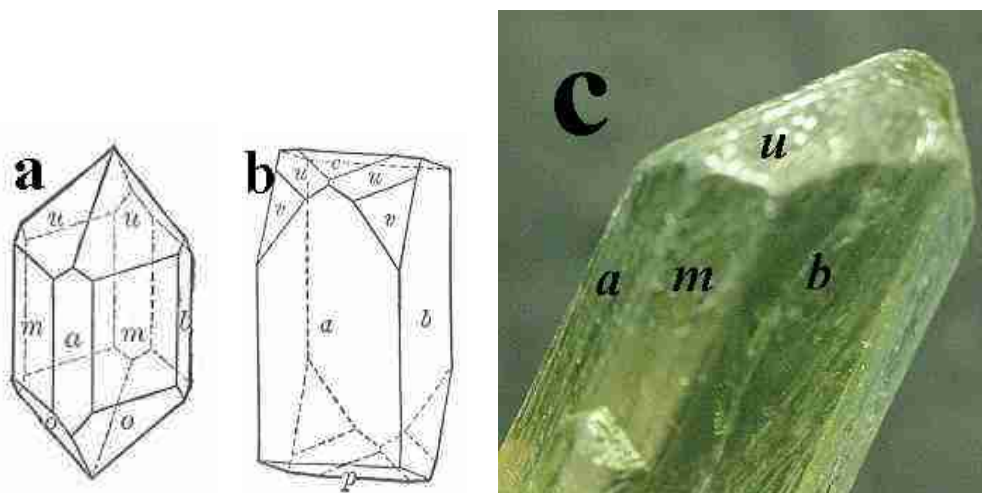


Figure 7. Clinopyroxene  $[(\text{Ca},\text{Mg},\text{Fe})\text{SiO}_3]$  displays several chiral faces (a and b), including the common (110) cleavage plane (designated *m*), and occasionally the (111), (221) and ( $\bar{2}21$ ) forms (designated *u*, *o*, and *v*, respectively). (c) The 1.3-cm diameter crystal of diopside ( $\text{CaMgSi}_2\text{O}_6$ ) from Xinjiang, Uygur Province, China, displays both the (110) and the (111) chiral forms.

Ambiguity arises when attempting to model the (110) surface structure of clinopyroxene. As in quartz and feldspar, the silicon atoms are assumed to remain tetrahedrally coordinated. The coordination of divalent cations, however, is less certain and will likely vary depending on the environment of the crystal. Figure 8 illustrates three different possible terminal atomic arrangements for the (110) surface of diopside. In the first configuration (Figure 8a and b) calcium atoms near the surface are coordinated to seven rather than eight oxygen atoms, thus exposing both positively-charged calcium and negatively-charged oxygen atoms at the surface.

Alternatively, magnesium may be partially coordinated near the surface in at least two possible configurations (Figure 8c through f). If Mg is four-coordinated near the surface, then a quasi-linear pattern of approximately planar surface atoms results (Figure 8c and d). If magnesium is five-coordinated near the surface, then a more complex surface structure results, with both positively-charged magnesium atoms and oxygen atoms at three different heights relative to the surface (Figure 8e and f). The adsorption characteristics of (110), consequently, will depend critically on the as yet unknown cation coordination at the surface.

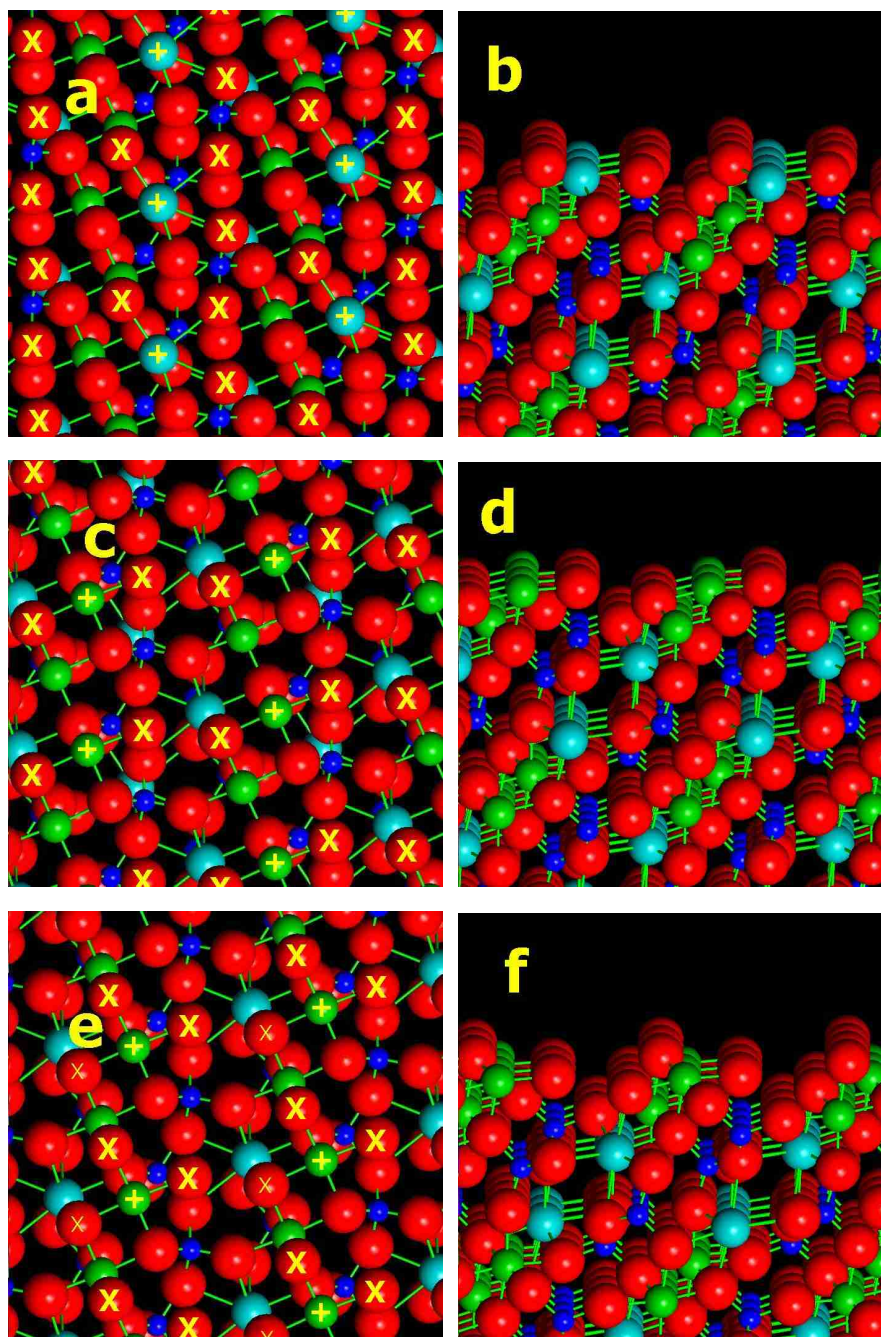


Figure 8. Three possible terminations for the (110) surface of diopside ( $\text{CaMgSi}_2\text{O}_6$ ). Ca, Mg, Si and O are turquoise, green, blue, and red, respectively. Each  $15 \times 15 \text{ \AA}$  drawing has the [001]-axis projection vertical. X and + indicate O atoms and cations near the surface. Small Xs in (e) are O atoms that are significantly below other surface atoms, but may participate in surface binding.

### 3.4 Calcite

Calcite ( $\text{CaCO}_3$ ; rhombohedral space group  $R\bar{3}c$ ), the principal mineral of limestone and marble, is of special interest in studies of chiral selection by mineral surfaces. Calcite was one of the most abundant marine minerals on the early Earth and calcite crystal surfaces would have been widely present in prebiotic environments [44,45]. Calcite is also one of the most common biominerals; it is strongly bonded to proteins in the shells of many invertebrates [46,47]. The potential for calcite to interact with chiral molecular species has been underscored by studies of surface growth topology, which may be strongly affected by the presence of L versus D amino acids [48].

The literature on calcite is confused by the common use of *four* different axial systems, each of which results in a different set of Miller indices for any given plane [36]. Two of these sets of axes are based on inconvenient rhombohedral unit cells (in which one axial length and one interaxial angle are specified). Most authors prefer the simpler hexagonal setting (in which two orthogonal axial lengths,  $a$  and  $c$ , are specified) and that convention is used in this chapter.

However, additional confusion arises from the existence of two different axial conventions for the hexagonal unit cell. One set of axes, based on the classic morphology of the calcite cleavage rhomb, results in the so-called “cleavage rhomb unit cell” or “morphological unit cell” ( $a = 10 \text{ \AA}$ ;  $c = 8.5 \text{ \AA}$  in the hexagonal setting). This cell is invariably used to describe twinning, cleavage, and crystal forms [36,37]. In this setting, the Miller indices for the common cleavage rhomb are (101). Alternatively, the so-called “structural unit-cell” ( $a = 5 \text{ \AA}$ ;  $c = 17 \text{ \AA}$  in the hexagonal setting) is the minimal unit cell determined by x-ray methods. In this case the axial orientations are identical to the morphological cell, but the  $a$  axis is halved and the  $c$  axis is doubled. Thus, for example, Miller indices for the cleavage face (101) in the hexagonal morphological setting become (104) in the hexagonal structural setting. When working with calcite surfaces, therefore, it is critical to specify both the unit cell and the Miller indices in order to avoid ambiguity.

The most common calcite crystal form is the scalenohedron, in which adjacent faces have mirror-related surface structures (Figure 9). This form, with Miller indices (211) in the hexagonal morphological cell or (214) in the structural cell, is of special interest because of its ability to adsorb D and L amino acids selectively [7]. Modeling the (211) scalenohedral surface is complicated by the nature of the calcite structure, which has a halite or NaCl-type face-centered cubic arrangement of alternating Ca cations and rigid  $\text{CO}_3$  anions. A few surfaces, such as the perfect rhombohedral cleavage [(101) or (104) in the morphological or structural settings, respectively], present a uniform surface structure of coplanar Ca and  $\text{CO}_3$  (Figure 10). This surface incorporates a glide plane operator and is thus achiral.

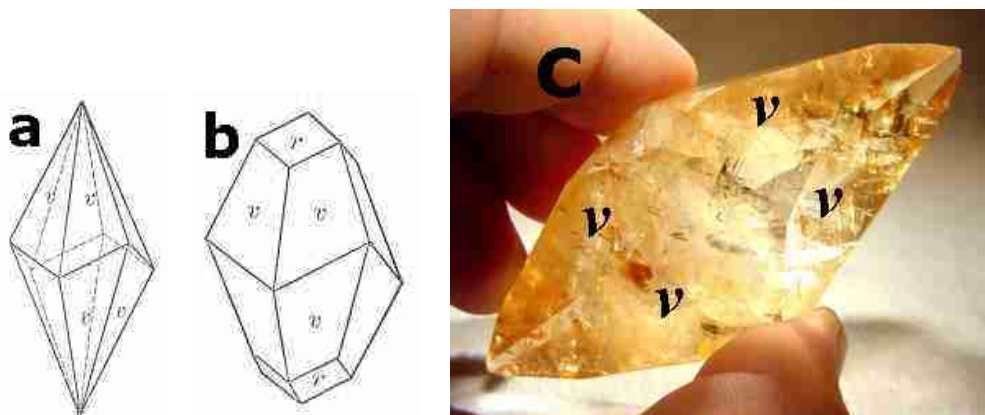


Figure 9. Calcite,  $\text{CaCO}_3$ , frequently occurs with (a) the chiral scalenohedral form [designated  $v$ ; (211) or (214) in the hexagonal morphological or structural setting, respectively], as well as (b) the rhombohedral form [designated  $r$ ; (101) or (104), respectively], which is also the common cleavage plane. (c) A doubly -terminated crystal from Elmwood Mine, Tennessee, displays a well -formed scalenohedron.

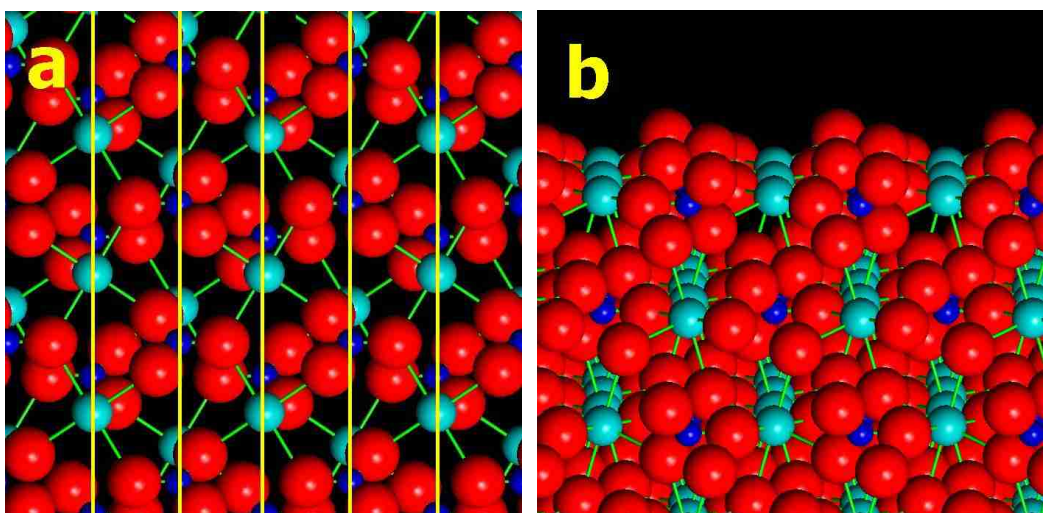


Figure 10. (a) The calcite rhombohedral cleavage [(101) or (104) in the hexagonal morphological or structural settings, respectively] presents a surface in which Ca cations and rigid  $\text{CO}_3$  anions alternate. The surface has glide plane symmetry (vertical yellow lines) and so is achiral. (b) The cleavage surface topology is revealed in a view that is tilted  $6^\circ$  from the horizontal. Ca, C and O atoms are turquoise, blue and red, respectively. Each drawing is approximately  $15 \times 15 \text{ \AA}$ , and the c-axis projections are vertical.

Most calcite crystal surfaces, however, intersect coplanar arrays of Ca and CO<sub>3</sub> groups so that the surface must incorporate steps and kinks, in much the same way as high-index planes of face-centered cubic metals are stepped and kinked [13]. Thus, the common calcite scalenohedral faces [(211) or (214) in the hexagonal morphological or structural settings, respectively] display a complex chiral surface topology that is not easily, or unambiguously, modeled.

Figure 11 displays a possible surface configuration, based on the assumption that all surface oxygen atoms are associated with CO<sub>3</sub> groups. This requirement leads to prominent 2-Å high surface steps (Figure 11b, arrow). These steps are parallel to  $[01\bar{8}]$  in the hexagonal structural setting (or  $[01\bar{2}]$  in the hexagonal morphological setting), and are spaced approximately 12 Å apart. This topology, with its linear array of chiral binding sites, may provide a natural template for the synthesis of homochiral polypeptides [7].

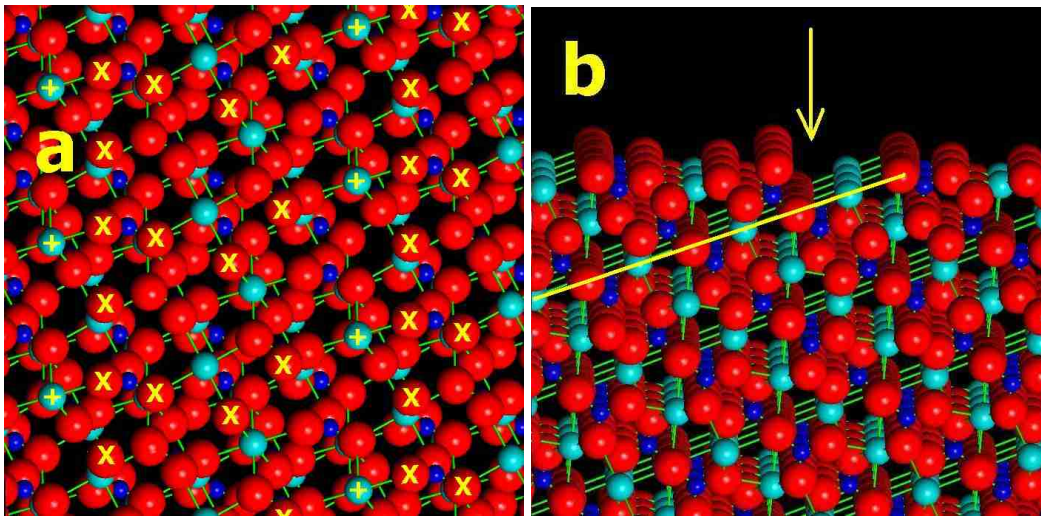


Figure 11. (a) The structure of the scalenohedral face of calcite [(211) or (214) in the hexagonal morphological or structural settings, respectively] features a chiral arrangement of positive (+) and negative (X) charge centers near the crystal termination. Ca, C and O atoms are turquoise, blue and red, respectively. In this 20 x 20 Å view the  $(01\bar{8})$  axis in the hexagonal structural setting [equivalent to the  $(01\bar{2})$  axis in the hexagonal morphological setting] is vertical – an orientation that provides a useful image of the surface structure. (b) A view of this surface tilted 3° from horizontal (projected almost down the  $[01\bar{8}]$  axis) reveals the irregular surface topology, including 2-Å-deep steps (yellow arrow) that result from the oblique intersection of layers of Ca and rigid CO<sub>3</sub> groups with the surface (yellow line).

### 3.5 Other Common Chiral Faces of Rock-Forming Minerals

In addition to quartz, feldspar, pyroxene and calcite, numerous other minerals display chiral surfaces. Most of these species are rare or their chiral forms are seldom expressed. However, two other particularly common minerals, amphibole and gypsum, deserve mention with regard to their common chiral crystal faces.

The amphibole minerals include a varied suite of hydrous chain silicates that are often found in igneous and metamorphic rocks [36]. This compositionally diverse group commonly conforms to the formula  $(\text{Na,K,Ca})_2(\text{Mg,Fe,Al})_5\text{Si}_8\text{O}_{22}(\text{OH})_2$ . Amphiboles are structurally related to pyroxenes and, like pyroxenes, occur in both orthorhombic and monoclinic forms. The latter clin amphibole group frequently displays chiral crystal faces and cleavage surfaces. These amphiboles, such as tremolite,  $\text{Ca}_2\text{Mg}_5\text{Si}_8\text{O}_{22}(\text{OH})_2$ , and actinolite,  $\text{Ca}_2(\text{Mg,Fe})_5\text{Si}_8\text{O}_{22}(\text{OH})_2$  (both monoclinic space group  $C2/m$ ;  $a = 9.8 \text{ \AA}$ ,  $b = 18.1 \text{ \AA}$ ,  $c = 5.3 \text{ \AA}$ ,  $\beta = 104.7^\circ$ ), routinely develop the chiral (110) and (011) forms, designated  $m$  and  $r$ , respectively, in Figure 12, as well as less common (120) form [37]. In addition, the (110) plane is a perfect cleavage in all clin amphibole species and so offers the potential for exposing fresh chiral surfaces for study. However, as with clinopyroxenes, the detailed surface structure of clin amphiboles will be strongly dependent on coordination of mono- and divalent cations at the surface. Further characterization of these faces thus represents a promising research opportunity.

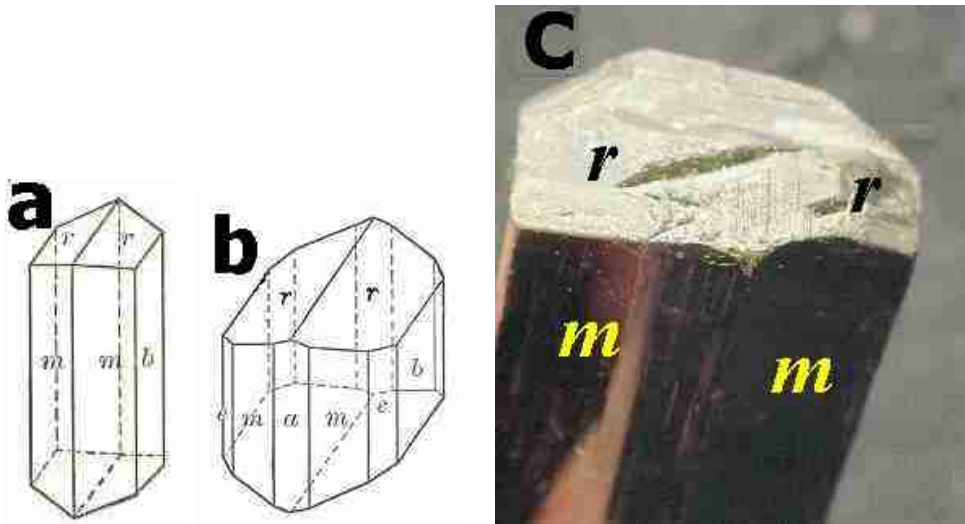


Figure 12. (a) The (110) and (011) forms of clin amphibole, designated  $m$  and  $r$ , respectively, are relatively common chiral crystal surfaces. (b) The chiral (120) form (designated  $e$ ) also occurs, though infrequently. (c) The 2-cm diameter crystal of actinolite [nominally  $\text{Ca}_2(\text{Mg,Fe})_5\text{Si}_8\text{O}_{22}(\text{OH})_2$ ] from Mpwa-Mpwa, Tanzania, displays both the  $m$  and  $r$  forms.

Gypsum ( $\text{CaSO}_4 \cdot 2\text{H}_2\text{O}$ ; monoclinic space group  $C2/c$ ;  $a = 5.7 \text{ \AA}$ ,  $b = 15.2 \text{ \AA}$ ,  $c = 6.3 \text{ \AA}$ ,  $\beta = 113.8^\circ$ ), the most abundant natural sulfate, is a common marine evaporite mineral that readily forms euhedral crystals with chiral (110) and (111) faces, as illustrated in Figure 13 [36,37]. Thick gypsum deposits are found around the globe in many regressive sedimentary sequences. Crystal growth is extremely rapid under appropriate evaporative conditions; natural euhedral crystals may achieve lengths in excess of 10 cm in several days (R.Lavinski, personal communications).

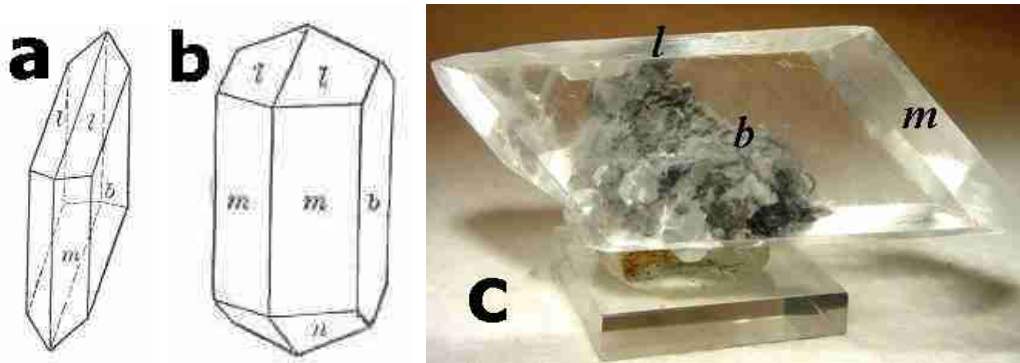


Figure 13. (a) Gypsum,  $\text{CaSO}_4 \cdot 2\text{H}_2\text{O}$ , commonly develops the chiral (110) and (111) forms, which are designated  $m$  and  $l$  respectively. (b) The  $(\bar{1}11)$  form (designated  $n$ ) is also seen occasionally. (c) A euhedral gypsum crystal from Gui Lin, Guanxi Province, China, 7.5 x 2.5 cm.

Gypsum has proven to be of special interest in studies of the interactions of chiral surfaces with chiral molecules. Growth of (110) and (111) faces, in particular, are dramatically influenced by the presence of chiral solute molecules [49]. Thus, for example, D and L alanine have been shown to thwart the growth of enantiomeric (110) faces, producing highly distorted crystals. This phenomenon has been invoked to explain the occurrence of uniformly asymmetric gypsum crystals from a Miocene evaporite deposit in Poland – an environment presumably dominated by L amino acids [50]. However, in spite of these intriguing morphological curiosities, the chiral surfaces of gypsum remain difficult to study because of the mineral's high degree of solubility in water.

#### 4. Conclusions

This brief overview points to several important conclusions regarding chiral crystalline surfaces.

1. *Chiral crystalline faces are ubiquitous in nature.* Quartz, feldspar, pyroxene, calcite, amphibole and gypsum provide a wealth of

enantiomeric atomic surfaces in virtually every common crustal rock on Earth and other terrestrial bodies. Furthermore, any irregular mineral fracture surface will provide an additional variety of local chiral environments. In addition, hundreds of other candidate crystal growth faces also occur in nature. Most of those surfaces occur either on relatively rare minerals [i.e., the (111) and (221) faces of topaz,  $\text{Al}_2\text{SiO}_4(\text{OH})_2$ , which occasionally forms crystals  $> 1$  m in length] or are crystal forms that are rare in well-developed specimens [i.e., the unusual (111) form of the common mineral olivine,  $(\text{Mg,Fe})_2\text{SiO}_4$ ]. A few of these less common surfaces will be present in most geochemical settings. Each of these surfaces has a specific atomic structure that represents a possible location for the selection, concentration and assembly of chiral organic species from the indiscriminately racemic prebiotic molecular soup into the homochiral macromolecules of life.

2. *Most mineral surfaces are not chiral:* With the exceptions of quartz (for which all crystal faces are inherently chiral) and calcite (for which the predominant scalenohedral face is chiral), most crystal growth surfaces on most minerals are achiral. Care must be taken, therefore, when studying minerals for their ability to induce chiral molecular separations. In this regard, special note should be made of layer hydroxides and layer silicates, including micas, chlorites and clays, which have been invoked in prebiotic processes of molecular selection and organization [51-54]. All layer silicates develop primarily the achiral (001) basal surfaces and therefore cannot impose a chiral environment.
3. *Different forms of a crystal typically display very different surface structures:* The (100), (101) and (011) forms of quartz are dramatically different. Each form has a different chiral surface distribution of atoms and a different atomic topography. Chiral interactions of molecules, therefore, are expected to differ for these different surfaces. In this regard it is significant that several previous experiments have employed powdered minerals (notably left- or right-handed quartz) in the hopes of inducing a chiral selective effect [2-5,55]. While such experiments may yield fortuitous enantiomeric excesses in the product suite, this use of powdered material greatly reduces the hope of discerning a structural mechanism for the observed chiral effect. The use of well-documented chiral crystalline surfaces is therefore much to be preferred.
4. *Some surfaces are "more chiral" than others:* The distribution of surface charges on some chiral faces, such as the (101) form of quartz, closely approximates an achiral configuration. Other faces, such as those of the calcite scalenohedron, deviate significantly from their enantiomer. These differences point to the possible utility of a "chirality index" that measures the misfit of a chiral surface with its enantiomer [56].

5. *In some instances the surface structure is ambiguous:* The surface structures of feldspar and clinopyroxene, for example, depend on the coordination numbers of monovalent and divalent cations at or near the surface – structural details that will depend strongly on the surface environment. Small changes in cation coordination can result in significant changes of the chiral surface charge distribution.
6. *So-called “flat” crystal faces may be stepped:* The surface of the calcite scalenohedron typifies an atomic configuration in which coplanar structural elements intersect a surface obliquely. This situation results in a stepped surface that may provide a linear array of chiral centers. Such an array may facilitate the condensation of homochiral polymers.

These distinctive attributes of chiral mineral surfaces point to significant opportunities for future studies at the dynamic interface between crystals and their environments.

## 5. Acknowledgements

I am grateful to Aravind Asthagiri, Robert Downs, Gözen Ertem, Mary Ewell, Andrew Gellman, James Kubicki, David Sholl and Henry Teng for useful discussions and constructive reviews of the manuscript. All crystal structure drawings were made with the program XtalDraw [57], courtesy of Robert Downs. Photographs of mineral specimens were generously supplied by Dr. Robert Lavinsky, President of Arkenstone in Garland, Texas.

## 6. References

- [1] R.M.Hazen and D.S.Sholl, *Nature Materials* 2 (2003) 367-374.
- [2] R.Tsuchida, M.Kobayashi and A.Nakamura, *J. Chem. Soc. Japan* 56 (1935), 1339-1341.
- [3] G.Karagounis and G.Coumoulos, *Nature* 142 (1938), 162-163.
- [4] A.Amariglio, H.Amariglio and X.Duval, *Helv. Chim. Acta* 51 (1968), 2110-2111.
- [5] W.A.Bonner, P.R.Kavasmaneck, F.S.Martin and J.J.Flores, *Origins of Life* 6 (1975), 367-376.
- [6] N.Lahav, *Biogenesis: Theories of Life's Origin*, Oxford University Press, NY, 1999.
- [7] R.M.Hazen, T.R.Filley and G.A.Goodfreind, *Proc. Natl. Acad. Sci. USA* 98 (2001), 5487-5490.
- [8] B. Kahr, S.Lovell and J.A.Subramony, *Chirality* 10 (1998), 66-71.
- [9] B.Kahr and R.W.Gurney, *Chem. Rev.* 101 (2001), 893-951.
- [10] S.C.Stinson, *Chem. Eng. News* 79 (May 14, 2001), 45-46.
- [11] M.Jacoby, *Chem. Eng. News* 80 (March 25, 2002), 43-46.
- [12] A.M.Rouhi, *Chem. Eng. News* 80 (June 10, 2002), 43-44.
- [13] C.F.McFadden, P.S.Cremer and A.J.Gellman *Langmuir* 12 (1996), 2483-2487.
- [14] D.S.Sholl, *Langmuir* 14 (1998), 862-867.
- [15] A.Ahmadi, G.Attard, J.Feliu and A.Rodes, *Langmuir* 15 (1999), 2420-2424.
- [16] G.A.Attard, *J. Phys. Chem. B* 105 (2001), 3158-3167.
- [17] D.S.Sholl, A.Asthagiri and T.D.Power, *J. Phys. Chem. B* 105 (2001), 4771-4782.
- [18] J.D.Horvath and A.J.Gellman, *J. Am. Chem. Soc.* 123 (2001), 7953-7954.

- [19] J.D.Horvath and A.J.Gellman, *J. Am. Chem. Soc.* 124 (2002), 2384-2392.
- [20] A.Kuhnle, T.R.Linderoth, B.Hammer and F.Besenbacher, *Nature* 415 (2002), 891-893.
- [21] Ž.Šljivančanin, K.V.Gothelf and B.Hammer, *J. Am. Chem. Soc.* 124 (2002), 14789-14794.
- [22] T.D.Power and D.S.Sholl, *Top. Catal.* 18 (2002), 201-208.
- [23] T.D.Power, A.Asthagiri and D.S.Sholl, *Langmuir* 18 (2002), 3737-3748.
- [24] F.J.Turner and J.Verhoogen, *Igneous and Metamorphic Petrology*, Mc-Graw-Hill, NY, 1960.
- [25] F.J.Pettijohn, *Sedimentary Rocks*, Harper & Row, NY, 1957.
- [26] F.D.Bloss, *Crystallography and Crystal Chemistry*, Holt, Reinhart and Winston, NY, 1971.
- [27] M.B.Boisen, Jr. and G.V.Gibbs, *Mathematical Crystallography*, Mineralogical Society of America, Washington, 1985.
- [28] L.Bragg, G.F.Claringbull and W.H.Taylor, *Crystal Structures of Minerals*, Cornell University Press, Ithaca, NY, 1965.
- [29] J.V.Smith, *Geometrical and Structural Crystallography*, John Wiley, NY, 1982.
- [30] C.Frondel, *Am. Mineral.* 63 (1978), 17-27.
- [31] E.Evgenii and T.Wolfram, *Origins Life Evol. Biosp.* 30 (2000), 431-434.
- [32] R.D.Murphy and T.M.El-Agez, *Indian J. Chem.* 35A (1996), 546-549.
- [33] B.L.Feringa and R.A.van Delden, *Angew. Chem. Int. Ed.* 38 (1999), 3418-3438.
- [34] D.Z.Lippmann and J.Dix, *Advances in Biochirality*, Eds. G.Palyi, C.Zucchi and L.Caglioti, Elsevier, Amsterdam, 1999, 85-98.
- [35] H.Zepik, E.Shavit, M.Tang, T.R.Jensen, K.Kjaer, G.Bolbach, L.Leiserowitz, I.Weissbuch and M.Lahav, *Science* 295 (2002), 1266-1269.
- [36] W.A.Deer, R.A.Howie and J.Zussman, *An Introduction to the Rock-Forming Minerals*. John Wiley, NY, 1971.
- [37] E.S.Dana, *A Textbook of Mineralogy*, John Wiley, NY, 1949.
- [38] R.Parsons, *Surface Sci.* 24 (1964), 418-826.
- [39] J.A.Davis and D.B.Kent, *Rev.Mineral.* 23 (1990), 177-259.
- [40] H.Churchill, H.Teng and R.M.Hazen, *Am. Mineral.*, in press.
- [41] M.C.Goldberg, E.R.Weiner and P.M.Boymel, *J. Chem. Soc. Faraday Trans.* 80 (1984), 1491-1498.
- [42] Y.Xiao and A.C.Lasaga, *Geochim. Cosmoch. Acta* 60 (1996), 2283-2295.
- [43] P.H.Ribbe, *Feldspar Mineralogy, 2<sup>nd</sup> Edition*, Mineralogical Society of America, Washington, DC, 1983.
- [44] A.W.Bailey and A.R.Palmer, Eds., *The Geology of North America: An Overview*, Geological Society of America, Boulder, Colorado, 1989.
- [45] D.W.Sumner, *Am. J. Sci.* 297 (1997), 455-487.
- [46] H.Lowenstam and S.Weiner, *On Biomineralization*, Oxford University Press, Oxford, UK, 1989.
- [47] S.Weiner and L.Addadi, *J. Mater. Chem.* 7 (1997), 689-702.
- [48] H.Teng, P.M.Dove, C.A.Orme and J.J.DeYoreo, *Science* 282 (1998), 724-727.
- [49] A.M.Cody and R.D.Cody, *J. Crystal Growth* 113 (1991), 508-519.
- [50] M.Babel, *Arch. Mineral.* 44 (1990), 103-135, plates 1-9.
- [51] A.G.Cairns-Smith, *Clay Minerals and the Origin of Life*. Cambridge University Press, 1986.
- [52] H.Hartman, G.Sposito, A.Yang, S.Manne, S.A.C.Gould and P.K.Hansma, *Clays & Clay Min.* 38 (1990), 337-342.
- [53] J.P.Ferris, C.-H.Huang and W.J.Hagan, Jr., *Origin Life Evol. Biosphere* 18 (1988), 121-128.
- [54] L.E.Orgel, *Origin Life Evol. Biosphere* 28 (1998), 227-234.
- [55] K.Soai, S.Osanai, K.Kadowaki, S.Yonekubo and I.Sato, *J. Am. Chem. Soc.* 121 (1999), 11235-11236.
- [56] R.T.Downs and R.M.Hazen, *J. Molec. Catal.*, in press.
- [57] R.T.Downs and M.Hall-Wallace, *Am.Mineral.* 88 (2003), 247-250.